[CANCER RESEARCH 61, 3853–3857, May 15, 2001]

Advances in Brief

In Vivo Evaluation of 5-[^{18}F]Fluoro-2′-deoxyuridine as Tracer for Positron Emission Tomography in a Murine Pancreatic Cancer Model

Ulrike Seitz,[1, 2] Martin Wagner,[1] Andreas T. Vogg, Gerhard Glatting, Bernd Neumaier, Florian R. Greten, Roland M. Schmid, and Sven N. Reske

Departments of Nuclear Medicine [U. S., A. T. V., G. G., B. N., S. N. R.] and Internal Medicine I [M. W., F. R. G., R. M. S.], University of Ulm, 89081 Ulm, Germany

Abstract

We used a murine tumor progression model for the evaluation of potential proliferation markers using positron emission tomography (PET). 5-[^{18}F]-2′-deoxyuridine ([^{18}F]FdUrd) was synthesized with >98% radiochemical purity and investigated in a pancreatic cancer model, transforming growth factor α transgenic mice crossbred to p53 deficient mice. Thymidylate synthase was increased already in premalignant lesions, whereas thymidine kinase 1 mRNA levels were up-regulated 4-fold in the pancreatic cancer specimen of these mice. PET imaging was performed after injection of 1 MBq of [^{18}F]FdUrd and 1 MBq of [^{18}F]fluoro-deoxyglucose. Animals with pancreatic cancer displayed focal uptake of both tracers. The [^{18}F]FdUrd uptake ratio closely correlated with the proliferation index as evaluated in morphometric and fluorescence-activated cell sorter analysis. These results indicate the potential of our tumor model for the evaluation of PET tracers and suggest [^{18}F]FdUrd as a tracer for the assessment of proliferation *in vivo*.

Introduction

Definitive animal models are of paramount importance for our understanding of biological processes and for the development of novel diagnostic and therapeutic strategies of human diseases. The biological relevance of currently used transplantation models in nude mice is limited (1). s.c. transplantation of malignant cells initiates tumors far distant from the natural side of the neoplasm. Furthermore, the lack of an intact immune system could alter pathophysiological characteristics of the neoplasm of even orthotopic implanted tumors. Finally, tumors developed from long-term cultured cancer cell lines might not represent the paternal tumor characteristics. In contrast, genetically engineered mouse models have proven to be a powerful tool to elucidate biological processes and to understand pathophysiological alterations of human diseases (1). We have described recently (2) a murine tumor progression model for ductal pancreatic cancer that recapitulates the cellular differentiation, the growth characteristics, and the genetic alterations of the human disease. In this model, pancreatic cancer develops from premalignant lesions in TGF-α[3] transgenic mice (3, 4). Crossbreeding these TGF-α transgenic mice to p53-deficient mice accelerates tumor development and results in pancreatic cancer development in a close time frame (2). Pancreatic cancer in humans has the worst prognosis of all of the gastrointestinal cancers because of late diagnosis and lack of effective treatment. The risk of pancreatic cancer increases steadily in patients with a long standing history of chronic pancreatitis (5). Current anatomically based imaging procedures like CT and endoscopic pancreaticography detect only indirect signs of invasive tumor growth such as a pancreatic mass or ductal abnormalities. [^{18}F]FDG has been shown to be more accurate than CT scanning in the differentiation of pancreatic adenocarcinoma from chronic pancreatitis (6, 7). It is currently accepted that an increased cellular influx of the glucose analogue [^{18}F]FDG, a higher rate of intracellular phosphorylation, and a negligible rate of dephosphorylation underlie the high uptake and sequestration of [^{18}F]FDG in cancer cells (8, 9). Inflammatory processes such as pancreatitis and abscesses take up [^{18}F]FDG avidly, and chronic pancreatitis is recognized as the most common reason for false positive [^{18}F]FDG-PET findings (10). Furthermore, [^{18}F]FDG uptake relates to the number of viable cells rather than to the tumor differentiation or the proliferative activity (11). In contrast to glucose, nucleosides are rapidly incorporated in DNA. [^{11}C]thymidine has been proposed as a radiotracer for imaging tumor proliferation with PET by several groups (12, 13). The clinical applications of [^{11}C]thymidine are limited because of its the rapid metabolism, the appearance of radiolabeled metabolites of thymidine, and the short half-life of [^{11}C]. The antineoplastic agent FdUrd is predominantly taken up by proliferating cells and phosphorylated to 5-fluoro-2′-deoxyUMP through the S-phase specific enzyme TK-1. Therefore, intracellular FdUrd uptake provides an indirect measurement of cellular TK-1 activity. 5-fluoro-2′-deoxyUMP binds irreversibly to the TS, resulting in an intracellular trapping of the thymidine analogue. High levels of TK-1 and TS have been reported in human breast cancer (14) and are associated with the S-phase fraction (15). In this study, we describe the automated synthesis of [^{18}F]FdUrd with high radiochemical purity and yield. The *in vivo* evaluation of [^{18}F]FdUrd as tracer for PET indicates a close correlation of tracer uptake and proliferative activity in our murine pancreatic tumor model.

Materials and Methods

Animals. The generation, genotyping, and phenotypic characterization of TGF-α transgenic mice (line #2261-3; Ref. 4) and p53-deficient mice (16) have been described. A detailed morphological and genetic analysis of the tumor progression in crossbred TGF-α transgenic and p53-deficient mice was published recently (2, 3). All of the experiments were performed according to the guidelines of the local Animal Care Committee.

Preparation of [^{18}F]FdUrd by Electrophile Fluorination. Carrier added [^{18}F]F_2 was produced by irradiating neon gas [Ne with 0.5% F_2 (40 μmol)] with 9-MeV deuterons by the ^{20}Ne(d, α) ^{18}F nuclear reaction. The irradiated gas was allowed to expand into a solution of 22 mg (70 μmol) of DiAcdUrd in 5 ml of 10% acetic acid in CH_2Cl_2. The solvent was evaporated, and the sealed reactor was heated to 130°C after adding 0.4 M phosphate buffer (pH 13). The reaction was neutralized with 0.5 M H_3PO_4, injected onto a Econosphere C18 column (Alltech, Deerfield, IL), and eluted with 0.15 M phosphate buffer (pH 6) at a flow rate of 20 ml/min. The elution time of [^{18}F]FdUrd was 12 min and 30 s, whereas the retention time was 4 min and 30 s for

Received 1/19/01; accepted 3/21/01.

The costs of publication of this article were defrayed in part by the payment of page charges. This article must therefore be hereby marked *advertisement* in accordance with 18 U.S.C. Section 1734 solely to indicate this fact.

[1] U. S. and M. W. contributed equally to this work.

[2] To whom requests for reprints should be addressed, at Department of Nuclear Medicine, University of Ulm, Robert-Koch-Strasse 8, D-89081 Ulm, Germany. Phone: 49-731-500-24509; Fax: 49-731-500-24979; E-mail: ulrike.seitz@medizin.uni-ulm.de.

[3] The abbreviations used are: TGF, transforming growth factor; CT, computerized X-ray tomography; [^{18}F]FDG, [^{18}F]fluoro-deoxyglucose; PET, positron emission tomography; FdUrd, 5-fluoro-2′-deoxyuridine; TK-1, thymidine kinase 1; TS, thymidylate synthase; DiAcdUrd, 3′,5′-di-*O*-acetyl-2′-deoxyuridine; HPLC, high-performance liquid chromatography; PCNA, proliferating cell nuclear antigen; BrdUrd, bromodeoxyuridine; FP, forward primer; RP, reverse primer.

[^{18}F]fluoride, 5 min and 40 s for [^{18}F]uracil, and 11 min for dUrd. The UV absorbance at 260 nm and the radioactivity were monitored simultaneously. The product fraction was filtrated and collected in 30 ml. Analytical HPLC (100 RP18 EC column; Merck, Darmstadt, Germany) was performed using 3% CH_3OH in 33 mM phosphate buffer (pH 8) at a flow rate of 1 ml/min. The eluent was changed to 30% CH_3OH in 33 mM phosphate buffer between 10 and 22 min. From 22 to 32 min, the initial eluent was used again. The observed retention times were 8 min and 50 s for FdUrd and 10 min 11 s for dUrd, simultaneously measuring radioactivity and UV at 260 nm.

Morphological Characterization. Animals were sacrificed 24 h after PET imaging and assessed for body weight and gross morphology. For light microscopy, pancreatic tissue was fixed in 4% phosphate-buffered paraformaldehyde for 12 h, embedded in paraffin, sectioned (4 μm), and stained with H&E. Immunohistochemical staining and counter staining for PCNA were performed as described previously (3). Specificity of PCNA staining was confirmed with *in vivo* BrdUrd labeling (2). Selected animals received injections with 1 ml/100 g BrdUrd solution (Amersham Pharmacia Biotech, United Kingdom) 3 h before sacrifice. Immunostaining for BrdUrd incorporation was performed on paraffin sections with a monoclonal anti-BrdUrd antibody following the manufacturer's recommendations (Boehringer Mannheim, Mannheim, Germany). Expression of murine TS (1) was evaluated on cryosections. In brief, sections were air-dried, fixed with 4% phosphate-buffered paraformaldehyde for 10 min, washed in PBS/0.05% Tween for 5 min followed by antigen unmasking (Vector Laboratories, Burlingame, CA), and sequentially treated with primary antibody (rabbit antiserum to recombinant human TS; a generous gift from Dr. G. W. Aherne, Institute of Cancer Research, Surrey, England) and Alexa568-labeled secondary antibody. The optimal dilutions and incubation times of primary antibodies were established in previous experiments. The sections were analyzed with confocal scanning laser microscopy.

Quantitative RNA Analysis. Quantification of the mRNA level was carried out using the ABI Prism 7700 Sequence Detection System (Taqman; Perkin-Elmer Applied Biosystems, Foster City, CA) in 180-day-old TGF-α transgenic mice before tumor development and in murine pancreatic cancer in relation to littermate controls. Differences were analyzed using the δ-δ-CT method (2). The following FPs, RPs, and primer concentrations were used:mTS-FP (300 nM), 5′-TACAGCCTGAGAGATGGAATTTCCTCT-3′; mTS-RP (300 nM), 5′-TTTATTTGTGGATCCCT-TGA-T-3′; mTK-1-FP (300 nM), 5′-AGGCTTTCGGCAGCATCTTG-3′; mTK-1-RP (150 nM), 5′-CGC-CAATCACCTCCACCT-CT-3′; murine cyclophilin-FP (300 nM), 5′-ATGGT-CAACCCCACCGTGT-3′; and murine cyclophilin-RP (300 nM), 5′-TTCT-GCTGTCTTTGGAACTTTGTC-3′. mRNA levels in TGF-α transgenics before tumor development and in murine pancreatic cancer were compared with 180-day-old littermate controls by the Mann-Whitney-Wilcoxon test. Differences were considered significant if $P < 0.05$.

PET Imaging and Evaluation. PET was performed using an ECAT EXACT HR+ tomograph (Siemens/CTI, Knoxville, TN) with an axial field of view of 15 cm (63 slices of 2.25-mm thickness). Mice were fasted for 8 h before undergoing PET. [^{18}F]FdUrd and [^{18}F]FDG were injected i.v. into a tail vein at a mean dose of 1 MBq at 2 consecutive days. Dynamic images (six frames over 1 min, six frames over 2 min, and three frames over 10 min) in two-dimensional mode were started immediately after the injection. No transmission scan was performed. Images were reconstructed using an iterative algorithm (17). The uptake in the pancreas was determined by a region of interest analysis and is given as ratio to the liver uptake.

Assessment of the Proliferation Index. For the proliferation index based on nuclear PCNA and BrdUrd staining, three sections separated at least 100 nm were analyzed for the number of positive nuclei in relation to the total number of nuclei. On average, 1686 $\pm$ 442 nuclei were analyzed for each section. The proportion of cells in S-phase was further determined by flow cytometry (18). Tissue samples were homogenized in lysis buffer [10 mM Tris (pH 7.4), 10 mM NaCl, 3 mM $MgCl_2$, 0.1 mM phenylmethylsulfonyl fluoride, and 5% NP40] followed by centrifugation at 400 $\times$ *g* for 10 min. The nuclear pellet was resuspended, fixed in ethanol, followed by RNase A treatment (200 μg/ml in 10 mM sodium citrate), stained with propidiumiodide (50 μg/ml), and analyzed using flow cytometry (FACSCALIBUR; Becton Dickinson, San José, CA). For each sample, 10,000 nuclei were analyzed in duplicate. Integrated and peak DNA signals were used for aggregate discrimination. To avoid cellular debris, events were gated out 1 log below the 2N DNA peak. Correlation between the proliferation index and the uptake ratio in the pancreatic region was analyzed by Pearson's multiple regression using Statistica (StatSoft, Inc., Tulsa, OK).

Results

Automated Synthesis of [^{18}F]FdUrd. [^{18}F]FdUrd was prepared from DiAcdUrd by electrophile fluorination in an automated synthesis unit within a total synthesis time of 60 min (Fig. 1*A*). The radiochemical purity of the radiopharmaceutical in isotonic solution was $>$ 98% with a chemical purity of $>$ 95% (UV) and a product volume of $<$ 30 ml. A typical HPLC quality control is depicted in Fig. 1*B*. The mean activity concentration was 15 MBq/ml, and the specific activity was about 20 GBq/mmol. The overall effective radiochemical yield was 10%, *i.e.*, 5 GBq of [^{18}F]F_2 resulted in 340 MBq of [^{18}F]FdUrd sufficient for *in vivo* PET imaging studies as described below.

mTK-1 and mTS Are Up-Regulated in Pancreatic Tumors in TGF-α Transgenic Mice. The pyrimidine analogue [^{18}F]FdUrd is intracellularly trapped after phosphorylation by the TK-1 and irreversibly interacts with TS. The mRNA expression of mTK1 and mTS was evaluated with real time PCR in TGF-α transgenic mice before tumor development (TGF-α, 180 days) as compared with littermate controls (wild type, 180 days). Furthermore, mRNA expression was quantified in pancreatic cancer specimen from TGF-α transgenic mice and animals crossbred to the p53-deficient background (tumor, TGF-α, TGF-α/p53+/−, and TGF-α/p53−/−) as described previously (2). Fig. 2*A* shows an up to 6-fold overexpression of mTK-1 mRNA in pancreatic tumors as compared with 180-day-old littermate control animals. This up-regulation was not evident before tumor development in TGF-α transgenic mice (*TGF-α*; Fig. 2*A*). The expression

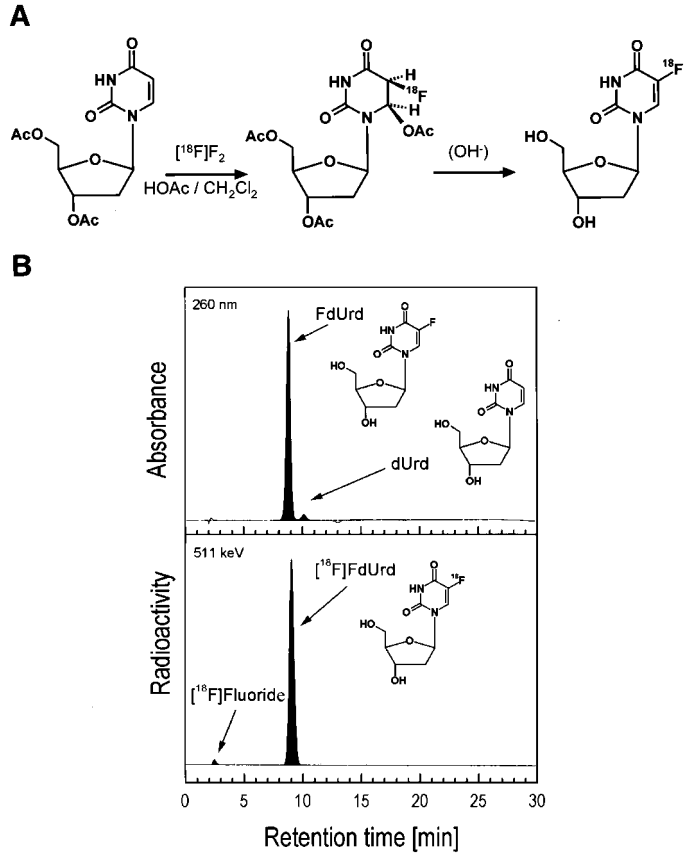

Fig. 1. Synthesis of [^{18}F]FdUrd from DiAcdUrd by electrophile fluorination (*A*). Analytic HPLC indicating the chemical purity (*top*, UV detection) and the radiochemical purity (*bottom*, γ detection) of [^{18}F]FdUrd (*B*). Synthesis resulted only in a minor fraction of unlabeled deoxyuridine (*dUrd*) and unbound fluoride ([^{18}*F*]).

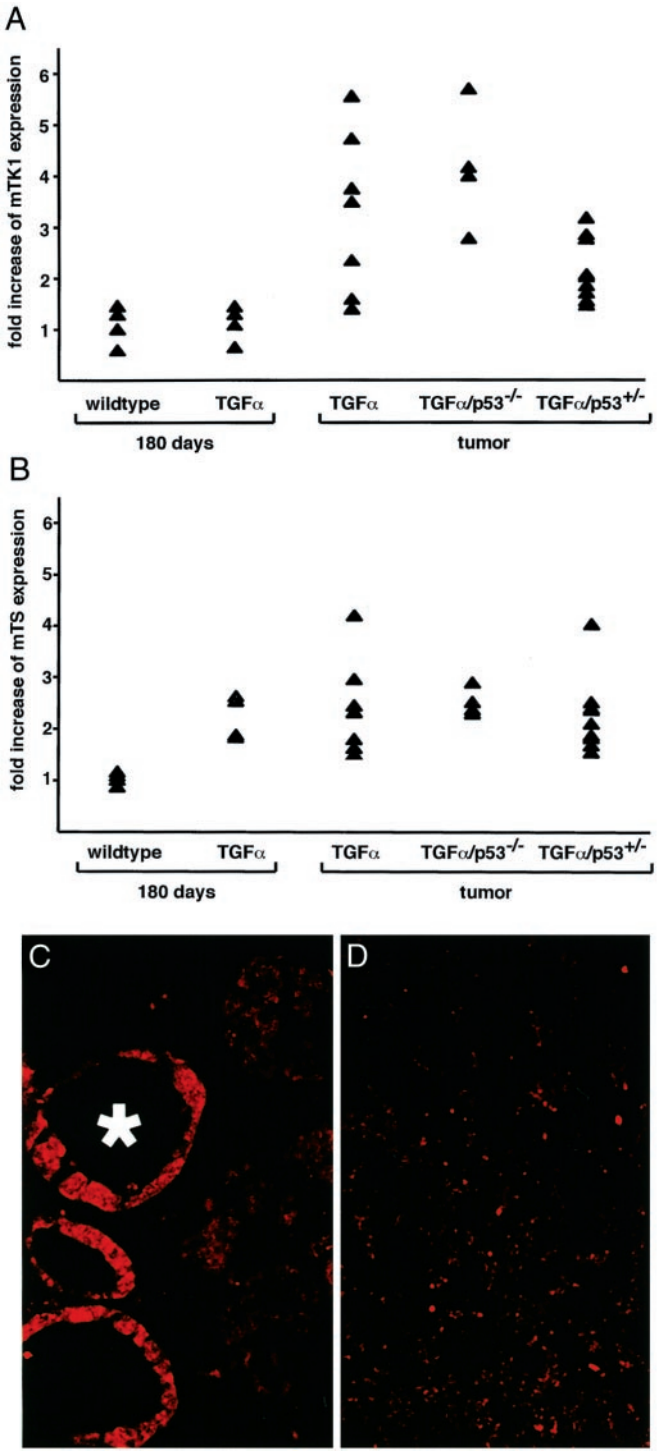

Fig. 2. Expression of mTK-1 mRNA (*A*) and mTS mRNA (*B*) in the pancreas of littermate controls (wild type, 180 days), transgenic animals before pancreatic cancer development (TGF-α, 180 days), and mice harboring pancreatic cancer (TGF-α, TGF-α/p53−/−, and TGF-α/p53+/−). mTK-1 mRNA level is up-regulated only in pancreatic cancer tissue (*A*). mTS is increased in the pancreas of TGF-α transgenic animals before tumor development (*B*). Each ▲ represents relative mRNA expression in an individual animal measured in triplicate. Values are normalized to endogenous cyclophilin expression and expressed as multiples of mean wild-type mRNA levels. Immunofluorescence staining shows mTS expression in premalignant ductal lesions of TGF-α transgenic mice (*C*, ∗) but no mTS expression in the surrounding acinar tissue or in littermate controls (*D*). Original magnification was ×150.

level of mTK-1 in pancreatic tumors arising in TGF-α transgenic animals varied from mRNA levels comparable with littermate controls to a 6-fold overexpression (Fig. 2*A*). Pancreatic tumors in TGF-α transgenic mice either heterozygote (TGFα/p53+/−) or homozygote (TGFα/p53−/−) deficient for the p53 gene displayed a comparable increase of mTK-1 mRNA levels with a more prominent up-regulation in homozygous p53-deficient mice (Fig. 2*A*). The increase in mRNA expression in tumor samples was significant as compared with wild-type controls and TGF-α transgenics before tumor development (Mann-Whitney-Wilcoxon test; $P < 0.05$). The mRNA level of mTS was significantly increased 2.5-fold already at the premalignant stage in the pancreas of TGF-α transgenic mice as compared with littermate controls (Fig. 2*B*; Mann-Whitney-Wilcoxon test; $P < 0.05$). Pancreatic cancers arising in TGF-α transgenic mice and the crossbred animals displayed a comparable increase of the mRNA level independent of the genotype (Fig. 2*B*). The up-regulation of mTS mRNA in TGF-α transgenic pancreas before the onset of malignant disease was further evaluated with immunofluorescence staining in 180-day-old TGF-α transgenic mice and littermate controls. Fig. 2*C* shows strong immunoreactivity for mTS in the tubular complexes (Fig. 2*C*; ∗) that represent the premalignant lesions in TGF-α transgenic mice. Only weak staining was detectable in the surrounding acinar and fibrotic tissue as well as in the pancreas of littermate controls (Fig. 2*D*).

PET Imaging with [^{18}F]FdUrd and [^{18}F]FDG as Tracers. PET imaging was performed in 24 animals including 180-day-old wild-type mice, 180-day-old TGF-α transgenics, and TGF-α transgenics crossbred to p53-deficient mice with suspected pancreatic cancer. Furthermore, 16 animals of this cohort were analyzed with both tracers on 2 consecutive days. The pancreatic uptake of both tracers was evaluated for each animal in a region of interest analysis and expressed as multiples of the liver uptake (see below) and the uptake to the brain as an additional control (data not shown). The [^{18}F]FdUrd uptake ratio in the pancreas ranged from 0.06 to 0.39. Focal pancreatic [^{18}F]FdUrd uptake (Fig. 3*A*, *arrow*; animal TGF-α/p53$^{+/-}$; pancreatic uptake ratio was 0.38) was evident in seven mice. Pancreatic cancer was confirmed in all of the seven cases. Macroscopically pancreatic tumors were separated from the surrounding fibrotic pancreas either as solid nodes (Fig. 3*C*, *arrow*) or as cystic formations with frequent intracystic bleeding (data not shown). Microscopic examination revealed cystic to papillary tumors and poorly differentiated tumors as described recently (2). The tumor in Fig. 3*D* formed small duct-like structures embedded in dense fibrotic tissue. Immunofluorescence staining with cytokeratin 19 confirmed the ductal differentiation of this tumor (data not shown). TGF-α transgenic mice without histological evidence of cancer displayed a diffuse, generalized uptake of [^{18}F]FdUrd in the pancreatic region of interest. In contrast, wild-type and p53-deficient controls negative for the transgene showed only weak accumulation of the tracer in the pancreatic region of interest. In all of the animals, we found pronounced uptake of [^{18}F]FdUrd in the liver and an accumulation of radioactivity in the kidney and the bladder (Fig. 3*A*).

Furthermore, 16 transgenic mice were sequentially analyzed with [^{18}F]FDG and [^{18}F]FdUrd PET. The [^{18}F]FDG uptake ratio in the pancreas ranged from 0.26 to 1.4. Focal pancreatic uptake of both tracers was evident in animals with histologically proven cancer (Fig. 3, *A* and *B*). The pancreatic uptake ratio in littermate controls showed great variation from 0.31 to 0.88 in the region of interest analysis. In addition, Fig. 3*B* shows uptake of [^{18}F]FDG in the brain, the heart, the liver, and the urinary tract. Comparable background activity was also present in littermate controls (data not shown).

Uptake Ratio of [^{18}F]FdUrd Correlates with Proliferation in TGF-α Transgenic Mice. Intracellular trapping of FdUrd is increased in proliferating cells (19). Therefore, we compared the [^{18}F]FdUrd uptake ratio obtained in a region of interest analysis with the proliferation index in TGF-α transgenic mice, animals with pancreatic cancer, and littermate controls. The proliferation index was deter-

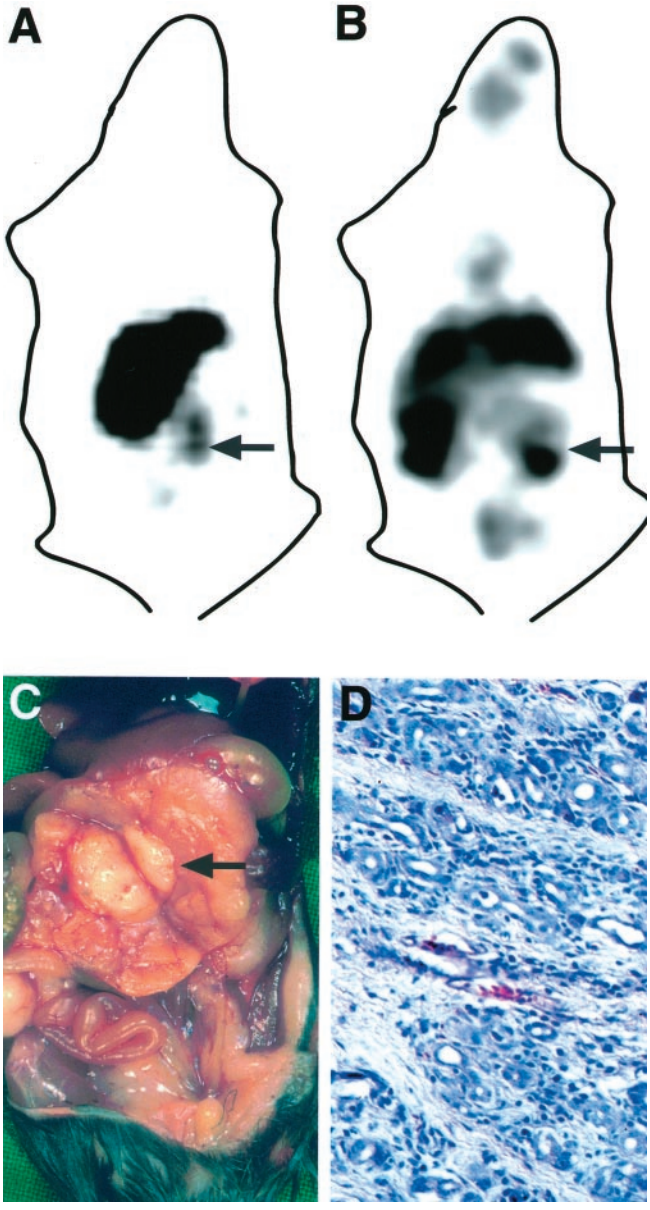

Fig. 3. Sequential PET imaging with [^{18}F]FdUrd (*A*) and [^{18}F]FDG (*B*) of animal #178 (genotype, TGF-α × p53−/−; age, 80 days) showing an increased uptake in the pancreatic region (*arrows*) with both tracers. Uptake of [^{18}F]FdUrd in the liver, the kidney, and the bladder is visible (*A*). The brain, heart, liver, and bladder show uptake of [^{18}F]FDG (*B*). Macroscopic examination reveals multiple tumor nodules in the fibrotic pancreas (*C, arrow*). Histological section confirms pancreatic cancer (*D*). H&E staining; original magnification was ×50.

mined from morphometric analysis of paraffin sections immunostained with PCNA antibodies. Comparable results were obtained with *in vivo* BrdUrd-labeling experiments in selected animals, confirming the specificity of the PCNA staining (data not shown). In addition, we analyzed tissue samples with flow cytometry after isolation of nuclei as described recently (18). The proportion of cells in S-phase measured by flow cytometry shows close correlation with our morphometric analysis ($r = 0.94$; $P > 0.0001$). The uptake ratio of [^{18}F]FdUrd in the pancreatic region closely correlates with the histological proliferation index (Fig. 4*A*). Multiple regression analysis resulted in a regression coefficient $r = 0.82$ ($P < 0.0001$). There was a definitive difference in the [^{18}F]FdUrd uptake ratio between TGF-α transgenic mice and animals with pancreatic cancer (Fig. 4*A*; ■) and the non-TGF-α transgenic littermates (Fig. 4*A*; ○). The correlation was less evident with [^{18}F]FDG as a tracer (Fig. 4*B*) resulting in a regression coefficient $r = 0.41$ ($P < 0.1$). In addition, there was a marked overlap of [^{18}F]FDG uptake ratio in littermate controls (○) and in TGF-α transgenic animals (■).

Discussion

This study demonstrates the ability of [^{18}F]FdUrd to image the proliferative activity of pancreatic cancer in a murine tumor model *in vivo*. The use of a genetically engineered mouse model in our study offers several advantages in comparison with *in vitro* experiments and currently used transplantation models. Tumors arise in the pancreas of immune competent animals and in a predictable time frame in TGF-α transgenic animals crossbred to p53-deficient mice (2). The invasive pancreatic cancer in our model closely resembles the human disease in terms of the ductal differentiation, a strong fibrotic reaction, and the genetic alterations involved in tumor progression (2). Pancreatic cancer develops from ductal cells within tubular complexes (3, 4). These tubular complexes display premalignant lesions in a dysplasia-carcinoma sequence (2). Immunofluorescence staining reveals that mTS is increased in these premalignant lesions. Furthermore, mTS mRNA is up-regulated 2.5-fold as evaluated in whole pancreatic lysates with real time PCR. This indicates a substantial increase of mTS in the premalignant lesions because tubular complexes represent only a minor cell fraction in the pancreas of 180-day-old TGF-α transgenic mice. In contrast, TK-1 is not up-regulated in tubular complexes and, thus, is only transcribed in the S-phase of the cell cycle (20). Our recent data indicate that overexpression of TGF-α promotes progression through G_1 but not S-phase in the pancreas of tumor-free TGF-α transgenic mice (2). As expected, mTK-1 mRNA levels are markedly increased in pancreatic tumors. This up-regulation does not depend on the genotype of mice and is detected in tumors of TGF-α transgenic

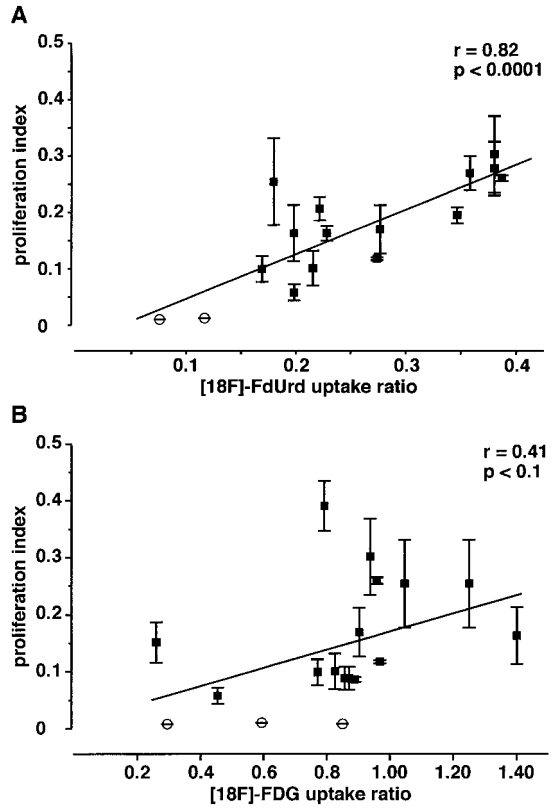

Fig. 4. Multiple regression analysis of the proliferation index, the [^{18}F]FdUrd (*A*) and [^{18}F]FDG (*B*) uptake ratio in the pancreatic region. Uptake of radioactivity was established in a region of interest analysis and expressed as multiples of liver uptake. ○, littermate controls; ■, TGF-α transgenic mice with and without pancreatic tumors.

mice, as well as in tumors of animals crossbred to p53-deficient mice. In addition, we found an up-regulation of TS and TK-1 in human pancreatic cancer specimen.[4] Moreover, increased levels of both enzymes have been reported in human breast cancer (14). These findings prompted us to evaluate [^{18}F]FdUrd as a potential proliferation marker for PET. Several strategies have been used recently (12, 21) to label thymidine and pyrimidine analogues as tracers for PET. [^{11}C]thymidine was successfully used in imaging proliferation of brain tumors; however, the general metabolic instability together with the short half-life of [^{11}C] limits the applications of this agent in clinical use (13). We established an automated synthesis for labeling FdUrd with [^{18}F] at the 5-position of the pyrimidine with high radiochemical purity and an overall yield suitable for PET studies. In our initial experiments, we compared PET scanning with [^{18}F]FdUrd and [^{18}F]FDG in our pancreatic tumor model. Pancreatic tumors displayed an increased focal uptake of [^{18}F]FDG as compared with the pancreatic region in littermate controls consistent with recent findings in human pancreatic cancer (6, 7). The uptake ratio of [^{18}F]FDG was comparable in the pancreas of tumor-free TGF-α transgenic animals with numerous tubular structures and in littermate controls. This suggested that [^{18}F]FDG PET was insufficient to detect premalignant changes in our model. Furthermore, the uptake of [^{18}F]FDG was not correlated with proliferation, confirming recent findings in human pancreatic cancer (22). In contrast, [^{18}F]FdUrd was already taken up in TGF-α transgenic mice containing tubular complexes but no tumors, indicating that increased expression of mTS might result in an intracellular accumulation of the tracer in these premalignant lesions. Focal uptake of [^{18}F]FdUrd was further increased in animals with evident pancreatic cancer. Most interestingly, there was a close correlation of [^{18}F]FdUrd uptake ratio with the proliferative activity, as evaluated by two independent methods. Thus, [^{18}F]FdUrd provides a noninvasive tool for the indirect measurement of proliferation in our pancreatic tumor model *in vivo*. This approach is limited by a pronounced uptake of [^{18}F]FdUrd in the liver, indicative for an accumulation of radiolabeled metabolites. This may be overcome using the following strategy. Because the uptake of [^{18}F]FdUrd in the liver is most likely attributable to its metabolic instability, labeling of more stable pyrimidine analogues is the subject of our current studies. The use of fluoride-substituted pyrimidine analogues increases the metabolic stability of these compounds, and recent findings (21) suggest [^{18}F]-3′-deoxy-3′fluorothymidine as a promising proliferation marker for PET studies. In summary, we developed a high yield synthesis for [^{18}F]FdUrd and evaluated this potential proliferation marker in a murine tumor model. The ability to measure proliferation *in vivo* by PET has direct impact for the clinical use in diagnosis and the surveillance of tumor development.

[4] Unpublished results.

References

1. Macleod, K. F., and Jacks, T. Insights into cancer from transgenic mouse models. J. Pathol., *187:* 43–60, 1999.
2. Wagner, M., Greten, F. R., Weber, C. K., Koschnik, S., Mattfeldt, T., Deppert, W., Kern, H., Adler, G., and Schmid, R. M. A murine tumor progression model for pancreatic cancer recapitulating the genetic alterations of the human disease. Genes Dev., *15:* 286–293, 2001.
3. Wagner, M., Lührs, H., Klöppel, G., Adler, G., and Schmid, R. M. Malignant transformation of duct-like cells originating from acini in transforming growth factor transgenic mice. Gastroenterology, *115:* 1254–1262, 1998.
4. Sandgren, E. P., Luetteke, N. C., Palmiter, R. D., Brinster, R. L., and Lee, D. C. Overexpression of TGFα in transgenic mice: induction of epithelial hyperplasia, pancreatic metaplasia, and carcinoma of the breast. Cell, *61:* 1121–1135, 1990.
5. Lowenfels, A. B., Maisonneuve, P., Cavallini, G., Ammann, R. W., Lankisch, P. G., Andersen, J. R., Dimagno, E. P., Andren Sandberg, A., and Domellof, L. Pancreatitis and the risk of pancreatic cancer. N. Engl. J. Med., *328:* 1433–1437, 1993.
6. Stollfuss, J. C., Glatting, G., Friess, H., Kocher, F., Berger, H. G., and Reske, S. N. 2-(fluorine-18)-fluoro-2-deoxy-D-glucose PET in detection of pancreatic cancer: value of quantitative image interpretation. Radiology, *195:* 339–344, 1995.
7. Inokuma, T., Tamaki, N., Torizuka, T., Fujita, T., Magata, Y., Yonekura, Y., Ohshio, G., Imamura, M., and Konishi, J. Value of fluorine-18-fluorodeoxyglucose and thallium-201 in the detection of pancreatic cancer. J. Nucl. Med., *36:* 229–235, 1995.
8. Goldberg, M. A., Lee, M. J., Fischman, A. J., Mueller, P. R., Alpert, N. M., and Thrall, J. H. Fluorodeoxyglucose PET of abdominal and pelvic neoplasms: potential role in oncologic imaging. Radiographics, *13:* 1047–1062, 1993.
9. Reske, S. N., Grillenberger, K. G., Glatting, G., Port, M., Hildebrandt, M., Gansauge, F., and Beger, H. G. Overexpression of glucose transporter 1 and increased FDG uptake in pancreatic carcinoma. J. Nucl. Med., *38:* 1344–1348, 1997.
10. Shreve, P. D. Focal fluorine-18 fluorodeoxyglucose accumulation in inflammatory pancreatic disease (see comments). Eur. J. Nucl. Med., *25:* 259–264, 1998.
11. Haberkorn, U., Ziegler, S. I., Oberdorfer, F., Trojan, H., Haag, D., Peschke, P., Berger, M. R., Altmann, A., and van Kaick, G. FDG uptake, tumor proliferation and expression of glycolysis associated genes in animal tumor models. Nucl. Med. Biol., *21:* 827–834, 1994.
12. Martiat, P., Ferrant, A., Labar, D., Cogneau, M., Bol, A., Michel, C., Michaux, J. L., and Sokal, G. *In vivo* measurement of carbon-11 thymidine uptake in non-Hodgkin's lymphoma using positron emission tomography. J. Nucl. Med., *29:* 1633–1637, 1988.
13. Eary, J. F., Mankoff, D. A., Spence, A. M., Berger, M. S., Olshen, A., Link, J. M., O'Sullivan, F., and Krohn, K. A. 2-[C-11]thymidine imaging of malignant brain tumors. Cancer Res., *59:* 615–621, 1999.
14. Sakamoto, S., Ebuchi, M., and Iwama, T. Relative activities of thymidylate synthetase and thymidine kinase in human mammary tumors. Anticancer Res., *13:* 205–207, 1993.
15. Sherley, J. L., and Kelly, T. J. Regulation of human thymidine kinase during the cell cycle. J. Biol. Chem., *263:* 8350–8358, 1988.
16. Jacks, T., Remington, L., Williams, B. O., Schmitt, E. M., Halachmi, S., Bronson, R. T., and Weinberg, R. A. Tumor spectrum analysis in p53-mutant mice. Curr. Biol., *4:* 1–7, 1994.
17. Schmidlin, P. Improved iterative image reconstruction using variable projection binning and abbreviated convolution. Eur. J. Nucl. Med., *21:* 930–936, 1994.
18. Casanova, M. L., Bravo, A., Ramirez, A., Morreale de Escobar, G., Were, F., Merlino, G., Vidal, M., and Jorcano, J. L. Exocrine pancreatic disorders in transgenic mice expressing human keratin 8. J. Clin. Investig., *103:* 1587–1595, 1999.
19. Crawford, E. J., Friedkin, M., Wolf, A. P., Fowler, J. S., Gallagher, B. M., Lambrecht, R. M., MacGregor, R. R., Shiue, C. Y., Wodinsky, I., and Goldin, A. 18F-5-Fluorouridine, a new probe for measuring the proliferation of tissue *in vivo*. Adv. Enzyme Regul., *20:* 3–22, 1982.
20. Romain, S., Martin, P. M., Klijn, J. G., van Putten, W. L., Look, M. P., Guirou, O., and Foekens, J. A. DNA-synthesis enzyme activity: a biological tool useful for predicting anti-metabolic drug sensitivity in breast cancer? Int. J. Cancer, *74:* 156–161, 1997.
21. Shields, A. F., Grierson, J. R., Dohmen, B. M., Machulla, H. J., Stayanoff, J. C., Lawhorn Crews, J. M., Obradovich, J. E., Muzik, O., and Mangner, T. J. Imaging proliferation *in vivo* with [F-18]FLT and positron emission tomography. Nat. Med., *4:* 1334–1336, 1998.
22. Buck, A., Schirrmeister, H., Guhlmann, A., Diederichs, C., Shen, C., Buchmann, I., Kotzerke, J., Birk, D., Mattfeldt, T., and Reske, S. N. Immunostaging in pancreatic cancer and chronic active pancreatitis: does *in vivo* FDG-uptake correlate with proliferative activity? J. Nucl. Med., in press, 2001.